

The Effects of Global Tidal Modes in a Non-hydrostatic Coupled Ionosphere-Thermosphere Model

Erdal Yiğit⁽¹⁾, Aaron J. Ridley⁽¹⁾

⁽¹⁾ *Department of Atmospheric, Oceanic and Space Sciences, University of Michigan
1429 Space Research Building, MI, 48109-2143, Ann Arbor, USA
erdal@umich.edu*

INTRODUCTION

Tides are one of the most studied types of atmospheric oscillations. In this work we consider large-scale solar thermal tides that have dynamical effects on the circulation of the upper atmosphere. Tidal oscillations are generated at different altitudes within the atmosphere. In the lower atmosphere, they are created by the absorption of solar EUV radiation by ozone and of infrared radiation by water vapour. They can be either *migrating* (Sun-synchronous) or *nonmigrating* propagating westward or eastward. Latent heat release associated with deep tropical clouds can generate nonmigrating tides. Tides have significant dynamical impact on the zonal mean circulation and produce composition variability at thermospheric altitudes [1; 2]. To assess the degree of vertical coupling in the atmosphere properly, it is crucial for general circulation models (GCMs) to account for the effects of these waves on the mean flow and their interactions with other types of waves of various scales. Most GCMs that are designed to study the upper atmosphere have lower boundaries situated either in the (lower) middle atmosphere [e.g., CMAT2, 3] or the lower thermosphere region [e.g., TIE-GCM, 4]. Besides the fact that some of these models possess sophisticated electrodynamics and neutral energetics, they lack an appropriate representation of the tidal waves originating from the lower atmosphere. Thus, they are forced at their lower boundaries in a variety of ways using empirical or theoretical models or datasets in order to incorporate the effects of lower atmospheric tidal variations on the upper atmosphere dynamics. For example, [5] uses the GSWM tidal fields in TIME-GCM to study possible effects of tidal variations and nonlinear effects among different wave components on the Mesosphere and Lower Thermosphere (MLT) and E-region dynamo.

Extending from the Earth's surface upwards, there are also coupled GCMs that can self-consistently generate lower atmospheric tides and simulate their effects in the upper atmosphere inherently. For example, WACCM3 demonstrates reasonable agreement with the Global Scale Wave Model (GSWM) and radar measurements of tidal fields [6].

We implement GSWM tidal fields at the lower boundary of the University of Michigan Global Ionosphere-Thermosphere Model (GITM) and study the effects of different tidal components on the upper atmosphere simulated by GITM. We compare these results to simulations performed by MSISE-90 lower boundary forcing. The paper is structured in the following way: Next section introduces the current version of GITM and implementation of the new GSWM lower boundary tidal forcing. We then describe the model setup and discuss the results. Finally, a brief summary and future work are presented.

MODEL DESCRIPTION AND IMPLEMENTATION OF TIDES

The Global Ionosphere-Thermosphere Model (GITM) is a non-hydrostatic 3-D first-principles based model extending from ~ 100 km to ~ 600 km. The model is described in detail in [7]. Here only some of the main features are briefly summarized. The vertical coordinate system is the altitude coordinate system instead of the pressure coordinate system used by traditional thermosphere models [e.g. 8]. This allows GITM to simulate dynamics of the upper atmosphere in a non-hydrostatic environment. The vertical momentum equation is explicitly solved. Reference [9] has shown that non-hydrostatic effects can play a significant role under intensive high-latitude Joule heating. Model resolution is flexible and the time step is around 2–4 s. By dividing the horizontal model domain into $n \times m$ latitudinal and longitudinal blocks, which are themselves composed of latitudinal and longitudinal cells, parallel computation is enabled. That is, the configured total number of blocks can be processed by multiple processors. Each block has typically 9 latitude x 9 longitude cells. Non-uniform grid in altitude and/or latitude can be used, which is referred to as grid stretching. This is useful, for example, for studying in detail the high-latitude dynamics under disturbed conditions. In our simulations, we use a uniform grid with $2.5^\circ \times 5.0^\circ$ latitude-longitude resolution and 54 altitude steps of $1/3$ scale height each.

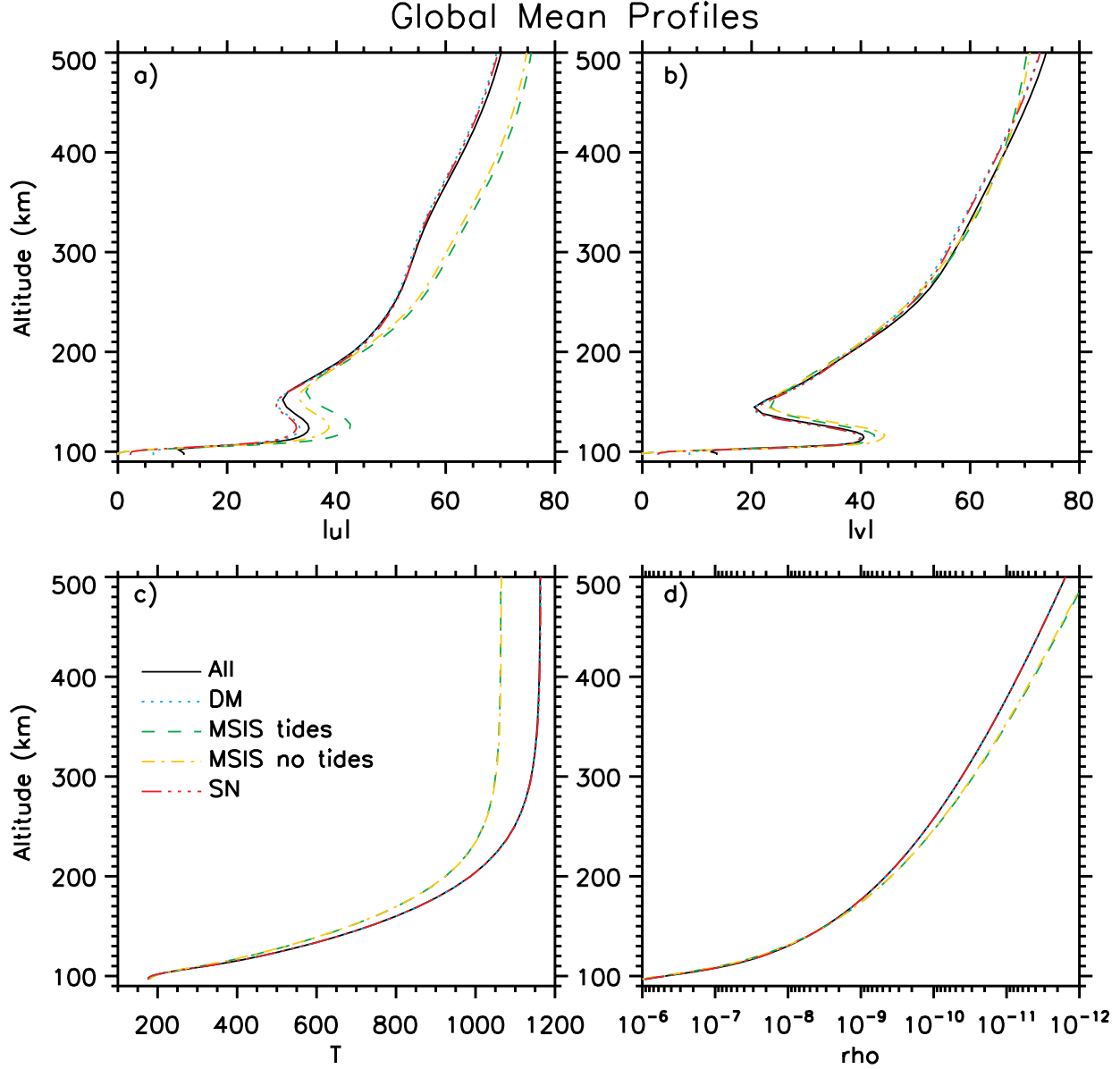


Fig. 1: Vertical profiles of global mean of a) zonal winds ($|u|$), b) meridional winds ($|v|$), c) neutral temperatures (T), and d) neutral densities ρ from 90 km up to 500 km. Black solid and green dashed lines denote EXP1 (GSWM all tidal components) and EXP0 (MSIS with tidal variations) simulations, respectively. Temperatures, winds, and densities are in K, m s^{-1} , and kg m^{-3} , respectively.

The model can be initialized using MSISE-90, IRI, and/or GSWM. GITM can also be run in 1-D. This is useful for quick model development. For the high-latitude electrodynamics a number of different models can be used [7, and references therein]. Neutral densities of O, O₂, N(²D), N(²D), S(²P), N₂, NO, H, and He; and ion species O⁺(²P), O₂⁺, N⁺, O⁺(⁴S), O⁺(²D), N₂⁺, NO⁺, H⁺, and He⁺ are explicitly calculated.

The standard version of GITM is initialized with zero zonal, meridional, and vertical winds (flat lower boundary); and MSISE-90 temperatures at the lower boundary. We will refer to this run as the benchmark run or EXP0 in the rest of the paper. EXP0 includes all MSISE-90 tidal variations. In order to study large-scale tides in the GITM thermosphere-ionosphere (TI), we implement GSWM [10] temperature perturbations and horizontal winds provided by Maura Hagan and Astrid Maute [private communication, 2009] at the GITM lower boundary. In a control file one can decide, which tidal components are to be used in a given GITM run. Cur-

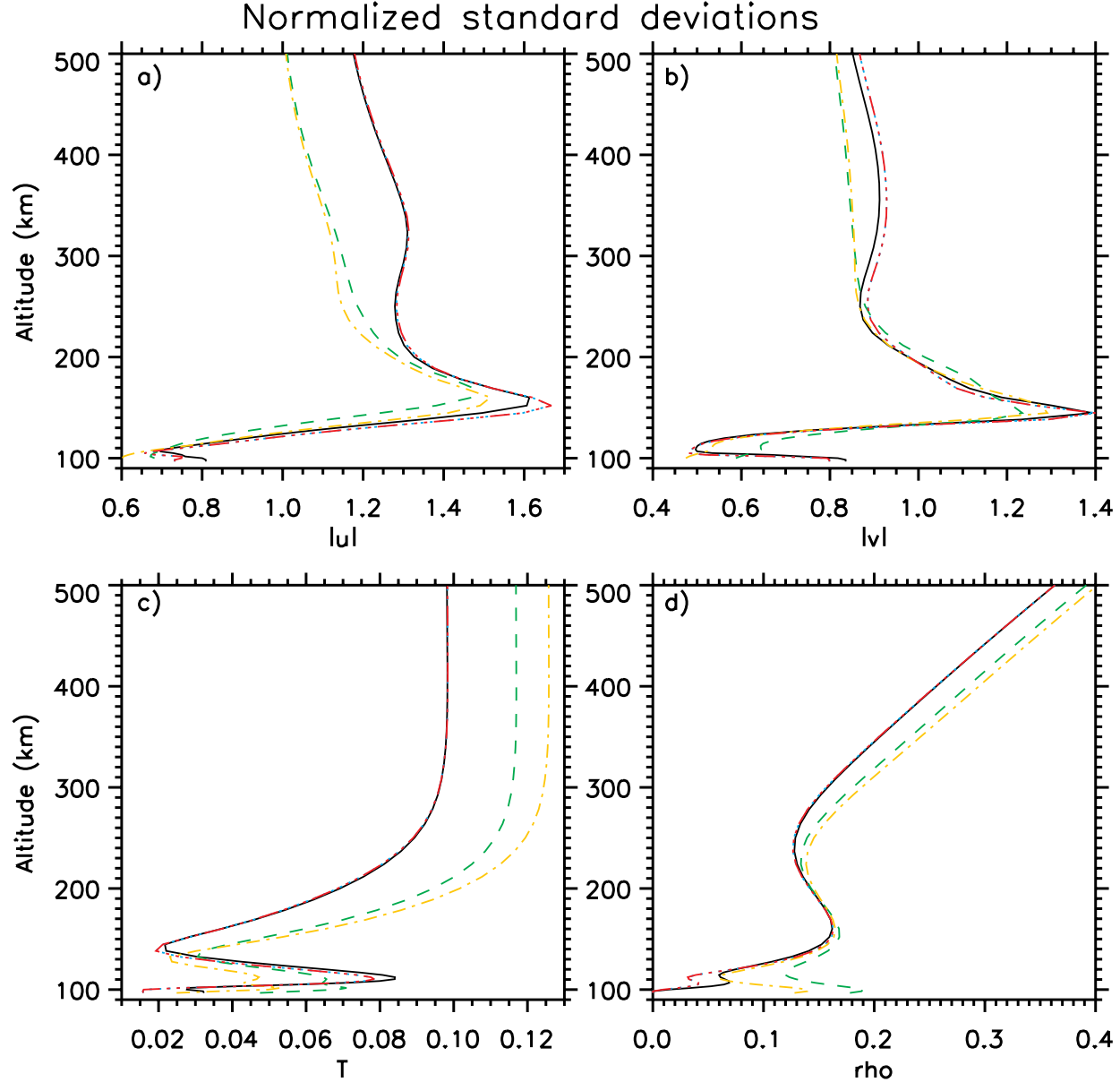


Fig. 2: Vertical profiles of normalized standard deviations of a) zonal winds (u), b) meridional winds (v), c) neutral temperatures (T), and d) neutral densities ρ . Each lower boundary forcing experiment is represented in the same way as in Fig. 1.

rently we have diurnal (DM) and semidiurnal migrating (SM); and diurnal (DN) and semidiurnal nonmigrating (SN) components. In particular, we will focus on the total effects of all GSWM tidal components and the comparison with the benchmark run. In the following section, we will describe the model setup used in this paper and present some of the preliminary results with different tidal components.

MODEL SETUP AND RESULTS

We have performed a series of simulations to test different lower boundary forcings in GITM and their effects in the upper atmosphere. The limited scope of this paper allows us to discuss only some cases in detail. All runs are at low geomagnetic and moderate solar activity (i.e. $F_{10.7} = 150 \text{ W m}^{-2} \text{ Hz}^{-1}$, $Kp = 1$). The following cases will be considered: i) MSIS tides (EXP0), ii) GSWM including all tidal components, i.e. DM+SM+DN+SN

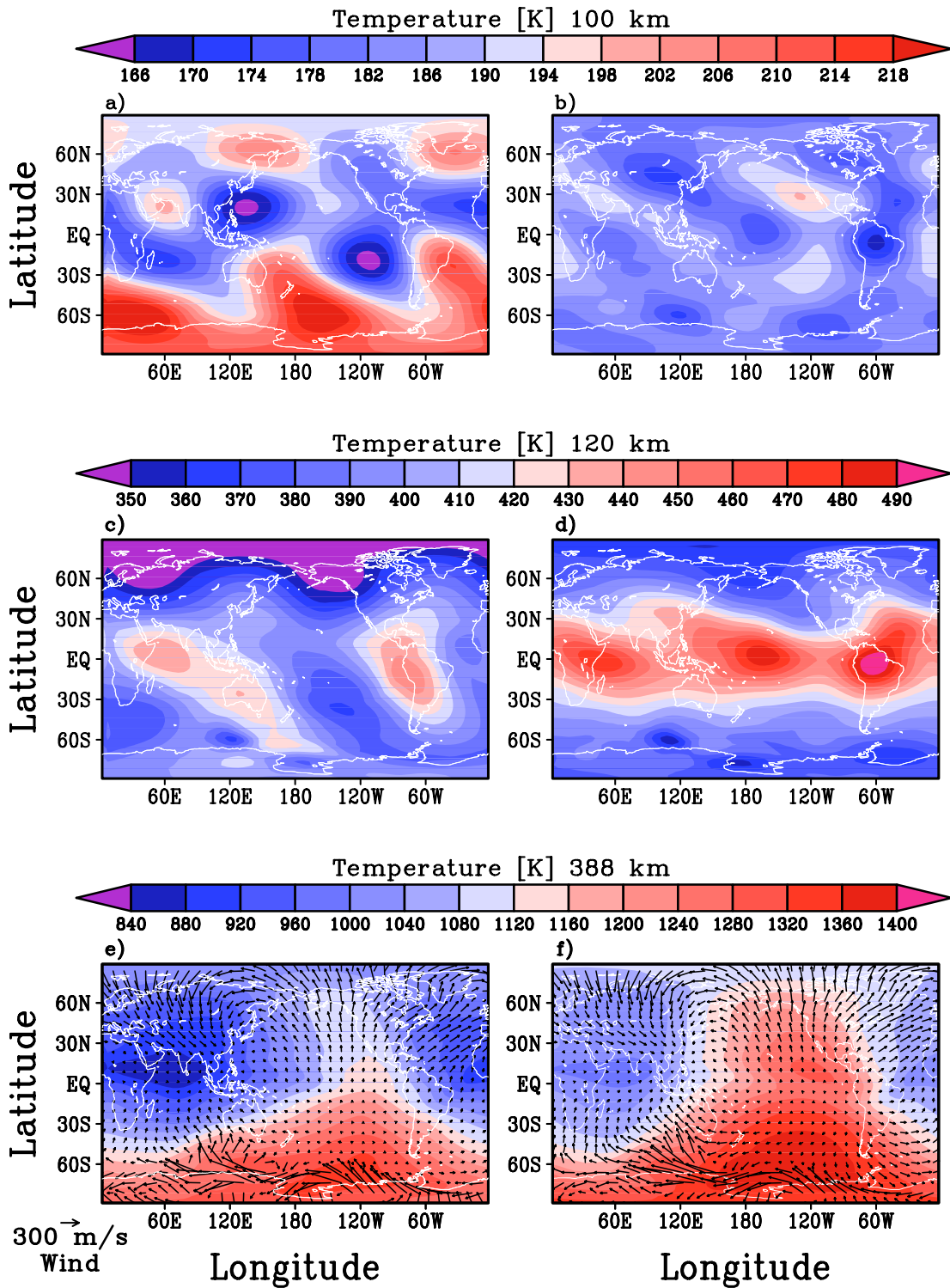


Fig. 3: Geographical distributions of the neutral temperatures on 23 December 2002, 0000 UT at three different altitude levels: The first column is the all tides run (EXP1) and the second column is the MSISE-90 tides run (EXP0). Rows one to three are the results at 100 km, 120 km, and 388 km, respectively. At each altitude the GSWM and the MSIS runs have been scaled with respect to the same color-scale. At 388 km the associated horizontal vector fields are overplotted with respect to the 300 m s^{-1} wind vector to demonstrate the morphology of the horizontal flow.

(EXP1), iii) MSIS without diurnal, semidiurnal, and terdiurnal variations, iv) GSWM diurnal migrating tide (DM), v) GSWM semidiurnal nonmigrating component (SN). GSWM tidal variations are interpolated every model time iteration. In each case GITM is run for 48 hours from 21 December 2002, 0000 UT till 23 December 2002, 0000 UT and the model outputs after 48 hours (i.e. on 23 December 2002 at 0000 UT) are analyzed. In the following section, we first present the global mean temperatures, neutral densities, and horizontal winds simulated with different lower boundary forcings.

Global Mean Profiles

First, we are interested in the amount of variations in globally averaged model parameters between different runs. For this, global mean temperatures \bar{T} , neutral densities $\bar{\rho}$, and horizontal winds $\bar{u} \equiv |\bar{\mathbf{u}}|$ and $\bar{v} \equiv |\bar{\mathbf{v}}|$ are evaluated on 23 December 2002, 0000 UT and their vertical profiles from 100 km to 500 km are shown in Figs. 1a–d. Different lines and colors are used to distinguish between different runs i)–v). It is seen that all the global mean profiles presented vary significantly from the lower to the upper thermosphere. In the global mean zonal and meridional winds the different lower boundary conditions are clearly seen at 100 km: The mean winds vary between 0 and ~ 15 m s $^{-1}$ with different lower boundary conditions (Figs. 1a–b). The absolute magnitudes of the winds increase up to ~ 70 – 75 m s $^{-1}$ in the upper thermosphere. Owing to intensive photoionization processes and inefficient radiative transfer in the thermosphere, the mean temperatures increase with altitude, too: from ~ 170 K to ~ 1050 – 1200 K. The mean neutral density decreases exponentially by a factor of 10^{-6} between 100 and 500 km.

Comparing all the runs to each other, overall we see increasing differences in the global mean temperature, wind and density profiles with increasing altitude between MSISE-90 lower boundary runs and GSWM ones. For example, the peak differences in \bar{u} seen between EXP0 and EXP1 in the upper thermosphere are in the order of 5 m s $^{-1}$. The associated differences in the global mean temperatures are about 100 K in the upper thermosphere. The mean zonal wind demonstrates additionally significant variation in the lower thermosphere at ~ 130 – 140 km, which is seemingly absent in the other model parameters presented. Besides the fact that there are clear differences between the effects of GSWM and MSISE-90 lower boundary forcings in GITM (EXP0 and EXP1, respectively), the variations among the effects of the different GSWM components on the global mean quantities are small.

In order to quantify the lower boundary induced fluctuations in T , $|\mathbf{u}|$, $|\mathbf{v}|$, and ρ , we have calculated the associated normalized standard deviations σ_u^N , σ_v^N , σ_T^N , and σ_ρ^N , for each simulation and plotted their vertical profiles in Fig. 2. The normalization for each parameter x is done with respect to its mean, \bar{x} : $\sigma_x^N \equiv \sigma_x/\bar{x}$.

Both the zonal and meridional winds demonstrate overall very large deviations from the mean in the thermosphere (Figs. 2a–b): 0.6–1.7 and 0.5–1.4 for σ_u^N and σ_v^N , respectively. It is noticeable that between 100 and 150 km both σ_u^N and σ_v^N increase overall by a factor of ~ 3 and then decrease with altitude. Analogous to the results presented in Fig. 1, there are significant differences between EXP0 and EXP1. GSWM lower boundary runs lead to larger oscillations around the global mean zonal and meridional winds than the benchmark run nearly at all altitudes. In the upper atmosphere, for example at 400 km, the $\sigma_{u,EXP1}^N$ is about 20% larger than $\sigma_{u,EXP0}^N$ and $\sigma_{v,EXP1}^N$ is $\sim 10\%$ more than $\sigma_{v,EXP0}^N$. In the lower thermosphere the differences are smaller except at 150 km for σ_u^N ; and 110 and 140 km for σ_v^N .

The associated temperature and density standard deviations, σ_T^N and σ_ρ^N , are much smaller than the winds (Figs 2c–d). With GSWM (EXP1) σ_T^N varies between 2% and 8.5% from 100 up to 500 km; and with MSISE-90 (EXP0) the associated variation is from 3% up to 11.5%. The standard deviations increase with altitude above ~ 150 km. Relatively large differences are seen between $\sigma_{\rho,EXP0}^N$ and $\sigma_{\rho,EXP1}^N$ at around 120 km (7%) and above 300 km $\sim 5\%$, where $\sigma_{\rho,EXP0}^N > \sigma_{\rho,EXP1}^N$.

Geographical Variations

In order to investigate some aspects of the variations seen in the global mean model parameters (Fig. 1) and their standard deviations (Fig. 2) further, we analyze the geographical distributions of the neutral temperatures in K at various altitude levels of interest. Fig. 3 illustrates latitude–longitude distributions of model tempera-

tures on 23 December 2002, 0000 UT at the model lower boundary (100 km, row 1), in the lower thermosphere (120 km, row 2) and the upper thermosphere (388 km, row 3) simulated in EXP0 (column 1) and EXP1 (column 2). At each altitude EXP0 and EXP1 results are presented with the same color scaling shown above the plots in each row. The color contour intervals are 4, 10, and 40 m s⁻¹ at 100, 120, and 388 km, respectively.

At the lower boundary, the benchmark run shows much larger temperature values, in particular at higher latitudes (Figs. 3a–b). Geographical variations of temperature values are larger than GSWM case, too. This is in agreement with $\sigma_{T,EXP0}^N > \sigma_{T,EXP1}^N$ at 100 km seen in Fig. 2c. At 120 km (Figs. 3c–d) however EXP1 has overall significantly larger temperatures, in particular at the equatorial regions. In the upper thermosphere (388 km, Figs. 3e–f) the differences in the magnitudes of temperatures and in the global distributions are still present. Again, GSWM lower boundary forcing leads to much larger upper thermospheric temperatures, as seen in Fig. 1c. For example, at the high-latitude summer thermosphere (70°S) the GSWM peak global temperature is ~60–70 K larger than the MSIS case: >1380 K vs. 1320 K. We have additionally overplotted the associated horizontal wind vector fields at 388 km with respect to the 300 m s⁻¹ wind vector. The effects of magnetospheric inputs in GITM are clearly seen, in particular, at the high-latitude summer hemisphere. The magnitude of the winds exceed 300 m s⁻¹. At high-latitudes fast winds are generated because the neutrals are forced by the ions that are controlled by the convection electric fields originating from the magnetosphere. Also a dominant summer to winter flow is apparent at 388 km. There are visible differences between EXP0 and EXP1 in the high-latitude summer hemisphere (60°W–60°E) in the magnitude and the direction of the horizontal flow.

Apparent differences seen between the benchmark run (EXP0) and GSWM-driven GITM (EXP1) are manifestations of the model sensitivity to the lower boundary specifications, which has to be taken into account in future modeling studies and comparison with observed datasets. We could see differences although we ran the model for a relatively short period of time of 2 days. Concerning the GSWM runs ii), iv), and v), we have seen minor variations among the effects of diurnal migrating, semi-diurnal nonmigrating and all tides cases on the global mean quantities and standard deviations. Analysis of longer model runs might be more conclusive regarding the individual and combined effects of different tidal components.

Summary and Future Work

Under low geomagnetic activity and moderate solar activity at solstice, we have used the 3-D Global Ionosphere-Thermosphere Model (GITM) in order to test different lower boundary forcing mechanisms based on the Global Scale Wave Model (GSWM) and MSISE-90. For this, different GSWM tidal components have been implemented at the GITM lower boundary (~100 km) to investigate different combinations of tidal effects. We have presented the global mean temperatures, neutral densities, zonal and meridional winds from 100 km to 500 km simulated under different lower boundary forcings, i.e. using MSISE-90 tides (EXP0), all GSWM tidal components (EXP1), diurnal migrating and semidiurnal nonmigrating GSWM tides, and MSISE-90 (no tides) boundary forcing. We have analyzed the standard deviations in these parameters. The global means and standard deviations have shown significant differences between EXP0 and EXP1. Finally, we have studied the geographical distributions of model temperatures at three different altitude levels: 100, 120, and 388 km. We have seen pronounced differences in the morphology of the temperatures at all altitudes. The differences in using MSISE-90 and GSWM as lower boundary conditions are likely to affect studies conducted with contemporary general circulation models.

We are planning to investigate in detail the individual effects of GSWM tidal components on the GITM upper atmosphere. We will be performing longer period model runs. UT and longitudinal variations in the context of high-latitude coupling can be studied. Sensitivity of the results to model resolution and thus to the amount of resolved eddies is also an important issue, which we will incorporate into our future studies. The upcoming ESA SWARM mission will provide large amount higher resolution geophysical data, which we will fruitful for interpreting GITM results further.

References

- [1] J. Oberheide and J. M. Forbes, “Thermospheric nitric oxide variability induced by nonmigrating tides,” *Geophys. Res. Lett.*, vol. 35, L16814, doi:10.1029/2008GL034825,2008.

- [2] J. M. Forbes, "Dynamics of the thermosphere," *J. Meteor. Soc. Japan*, vol. 85B, pp. 193, 213, 2007.
- [3] E. Yiğit, A. S. Medvedev, A. D. Aylward, P. Hartogh, and M. J. Harris, "Modeling the effects of gravity wave momentum deposition on the general circulation above the turbopause," *J. Geophys. Res.*, vol. 114, D07101, doi:10.1029/2008JD011132, 2009.
- [4] A. D. Richmond and E. C. Ridley, "A thermosphere/ionosphere general circulation model with coupled electrodynamics," *Geophys. Res. Lett.*, vol. 19, pp. 601–604, 1992.
- [5] M. E. Hagan, A. Maute, and R. G. Roble, "Tropospheric tidal effects on the middle and upper atmosphere," *J. Geophys. Res.*, vol. 114, A01302, doi:10.1029/2008JA013637, 2009.
- [6] L. Chang, S. Palo, M. Hagan, J. Richter, R. Garcia, D. Riggin, D. Fritts, "Structure of the migrating diurnal tide in the Whole Atmosphere Community Climate Model (WACCM)," *Adv. Sp. Res.*, vol. 41, pp. 1398–1407, 2008.
- [7] A. J. Ridley, Y. Deng, and G. Tóth, "The global ionosphere–thermosphere model," *J. Atmos. Sol.-Terr. Phys.*, vol. 68, pp. 839–864, 2006.
- [8] T. J. Fuller-Rowell and D. Rees, "A three-dimensional time-dependent, global model of the thermosphere," *J. Atmos. Sci.*, vol. 37, pp. 2545–2567, 1980.
- [9] Y. Deng, A. D. Richmond, A. J. Ridley, and H. Liu, "Assessment of the non-hydrostatic effect on the upper atmosphere using a general circulation model (GCM)," *Geophys. Res. Lett.*, vol. 35, L01104, doi:10.1029/2007GL032182, 2008.
- [10] M. E. Hagan and J. M. Forbes, "Migrating and nonmigrating semidiurnal tides in the middle and upper atmosphere excited by tropospheric latent heat release," *J. Geophys. Res.*, vol. 108(A2), doi:10.1029/2002JA009466, 2003.